



ELSEVIER

Contents lists available at ScienceDirect

Journal of Ginseng Research

journal homepage: <https://www.sciencedirect.com/journal/journal-of-ginseng-research>

Ginsenoside Rh2 reduces m6A RNA methylation in cancer via the KIF26B-SRF positive feedback loop

Chunmei Hu^{a,1}, Linhan Yang^{d,1}, Yi Wang^e, Shijie Zhou^{f,*}, Jing Luo^{c,**}, Yi Gu^{b,***}^a Department of Otolaryngology-Head and Neck Surgery, Sichuan Provincial People's Hospital, University of Electronic Science and Technology of China, Chengdu, Sichuan, China^b Department of Vascular and Thyroid Surgery, Sichuan Provincial People's Hospital, University of Electronic Science and Technology of China, Chengdu, Sichuan, China^c Department of Breast Surgery, Sichuan Provincial People's Hospital, University of Electronic Science and Technology of China, Chengdu, Sichuan, China^d Outpatient Department, Chengdu Aurora Huan Hua Xiang, Chengdu, Sichuan, China^e Department of Specialty of Geriatric Endocrinology, Sichuan Provincial People's Hospital, University of Electronic Science and Technology of China, Chengdu, Sichuan, China^f State Key Laboratory of Biotherapy and Cancer Center, West China Hospital, Sichuan University and Collaborative Innovation Center, Chengdu, Sichuan, China

ARTICLE INFO

Article history:

Received 24 March 2021

Received in revised form

11 May 2021

Accepted 12 May 2021

Available online 25 May 2021

Keywords:

ginsenoside Rh2

KIF26B

SRF

m6A RNA methylation

Cancer

ABSTRACT

Background: The underlying mechanisms of the potential tumor-suppressive effects of ginsenoside Rh2 are complex. N6-methyladenosine (m6A) RNA methylation is usually dysregulated in cancer. This study explored the regulatory effect of ginsenoside Rh2 on m6A RNA methylation in cancer.

Methods: m6A RNA quantification and gene-specific m6A RIP-qPCR assays were applied to assess total and gene-specific m6A RNA levels. Co-immunoprecipitation, fractionation western blotting, and immunofluorescence staining were performed to detect protein interactions and distribution. QRT-PCR, dual-luciferase, and ChIP-qPCR assays were conducted to check the transcriptional regulation.

Results: Ginsenoside Rh2 reduces m6A RNA methylation and *KIF26B* expression in a dose-dependent manner in some cancers. *KIF26B* interacts with *ZC3H13* and *CBLL1* in the cytoplasm of cancer cells and enhances their nuclear distribution. *KIF26B* inhibition reduces m6A RNA methylation level in cancer cells. SRF bound to the *KIF26B* promoter and activated its transcription. *SRF* mRNA m6A abundance significantly decreased upon *KIF26B* silencing. *SRF* knockdown suppressed cancer cell proliferation and growth both *in vitro* and *in vivo*, the effect of which was partly rescued by *KIF26B* overexpression.

Conclusion: ginsenoside Rh2 reduces m6A RNA methylation via downregulating *KIF26B* expression in some cancer cells. *KIF26B* elevates m6A RNA methylation via enhancing *ZC3H13/CBLL1* nuclear localization. *KIF26B*-SRF forms a positive feedback loop facilitating tumor growth.

© 2021 The Korean Society of Ginseng. Publishing services by Elsevier B.V. This is an open access article under the CC BY-NC-ND license (<http://creativecommons.org/licenses/by-nc-nd/4.0/>).

* Corresponding author. State Key Laboratory of Biotherapy and Cancer Center, West China Hospital, Sichuan University and Collaborative Innovation Center, Chengdu, 610041, Sichuan, China

** Corresponding author. Department of Breast Surgery, Sichuan Provincial People's Hospital, University of Electronic Science and Technology of China, Chengdu, 610072, Sichuan, China

*** Corresponding author. Department of Vascular and Thyroid Surgery, Sichuan Provincial People's Hospital, University of Electronic Science and Technology of China, Chengdu, 610072, Sichuan, China

E-mail addresses: vicjaychou@hotmail.com (S. Zhou), jingluo66@sina.com (J. Luo), scphguyi@21cn.com (Y. Gu).

¹ Chunmei Hu and Linhan Yang contributed equally to this study.

1. Introduction

Ginsenosides are a group of critical active chemical compounds of Ginseng (*Panax ginseng* Mey). Ginsenoside Rh2 is a metabolite of Rg3, Rb1, Rb2, and Rc, which shows stronger tumor-suppressive effects than the parental compounds [1]. The underlying mechanisms are multifaceted. It induces G1 phase cell cycle arrest and apoptosis via activating p53 inhibiting PDZ-binding kinase/T-LAK cell-originated protein kinase (PBK/TOPK) pathway [2–4]. This compound also participates in some epigenetic processes, such as DNA methylation [5,6].

N6-methyladenosine (m6A) RNA methylation is the most abundant mRNA internal modification regulating gene

transcription, translation, metabolism, and processing in diverse physiological processes [7]. It is a reversible and dynamic biological process regulated by multiple protein complexes termed as "writers", "readers" and "erasers". The writer complex comprises the core N6-adenosine methyltransferases methyltransferase-like 3 (METTL3), METTL14 and several adaptors, including Wilms' tumor-associated protein (WTAP), VIRILIZER (also called Virma), Cbl proto-oncogene like 1 (CBLL1), RNA binding motif protein 15 (RBM15), and zinc finger CCH-type containing 13 (ZC3H13) [8]. RNA methyltransferases, demethylases, and m6A binding proteins are frequently dysregulated in human tumors [8]. Their aberrant expressions are associated with increased expression of oncogene transcripts and oncoproteins [8]. However, whether ginsenoside Rh2 is involved in m6A RNA regulation is still not clear.

Kinesin family member 26B (KIF26B) is a member of the kinesin motor proteins, which transports organelles along microtubules [9]. It acts as a novel oncogene in multiple tumors, including colorectal cancer, gastric cancer, sarcoma, and breast cancer [10–12]. KIF26B upregulation activates multiple genes in the vascular endothelial growth factor (VEGF) pathway, such as *VEGFA*, *PXN*, *FAK*, *PIK3CA*, *BCL2*, and *CREB1* in gastric cancer [12]. Interestingly, the stability and translation of *VEGFA* and *BCL2* in some cancers are enhanced by m6A RNA methylation [13,14]. These findings imply that KIF26B might participate in m6A RNA methylation in cancer.

This study explored the modulation of ginsenoside Rh2 on m6A RNA levels in cancer and the underlying mechanisms.

2. Materials and methods

2.1. Retrospective bioinformatic analysis

RNA-seq data from The Cancer Genome Atlas (TCGA) and the Genotype-Tissue Expression (GTEx) project were acquired and analyzed using GEPIA2 [15] and UCSC Xena Browser [16].

2.2. Cell culture and treatment

Breast cancer cell line MDA-MB-157 and MCF-7 and sarcoma cell line SK-LMS-1 were obtained from ATCC (Manassas, MA, USA). Thyroid cancer cell line 8305C and TT, lung cancer cell line NCIH226, NCIH1299, and NCIH1650 were obtained from the National Collection of Authenticated Cell Cultures, China. Sarcoma cell line KYM-1 and NMFH-1 were obtained from RIKEN Cell Bank (Japan). The cells were cultured in DMEM or RPMI-1640 medium supplemented with 10% fetal bovine serum (FBS), according to the providers' instruction.

Lentiviral particles carrying shRNAs were constructed with the pLKO.1-puro plasmid. Lentiviral expression vectors were generated using the pHBLV-CMVIE-IRES plasmids. The following lentiviruses were generated, including lentiviral shRNA targeting *KIF26B* (shKIF26B) and *SRF* (shSRF), lentiviral *KIF26B* (NM_018012.4) expression vector with HA tag (HA-KIF26B), lentiviral *KIF26B* expression vector that was resistant to shKIF26B#1 (by synonymous mutation, MT-KIF26B), lentiviral full-length *ZC3H13* (NM_001076788.2) and truncated vectors (Δ C879, Δ N789, Δ C1024 and Δ N644) with N-terminal Flag tag (Flag-ZC3H13), lentiviral full-length *CBLL1* (NM_024814.4) and truncated vectors (Δ C344, Δ N147, Δ C285 and Δ N206) with N-terminal Flag tag (Flag-CBLL1), and *SRF* (NM_003131.3) expression plasmids.

ShRNA sequences were provided in Table S2. Lentiviruses were produced by co-transfecting the plasmids with packaging plasmids (pSPAX2 and pMD2.G) (HanBio Technology) in 293T cells using Lipofectamine 2000 (Invitrogen, Carlsbad, CA, USA) according to the manufacturer's instructions. Cells were infected with each

lentivirus supernatant at the multiplicity of infection (MOI) of 10 (Sigma-Aldrich, St Louis, MO, USA).

Ginsenoside Rh2 was purchased from MedChemExpress (Purity \geq 98%, Shanghai, China). Transcriptional inhibition was conducted by using actinomycin D (5 μ g/mL; catalog #HY-17559; Sigma-Aldrich) 24 h after lentiviral infection. After 0, 1.5, or 3 h treatment, cells were harvested for reverse-transcription quantitative real-time-PCR (qRT-PCR) analysis.

2.3. Immunofluorescence (IF) staining

Cells were rinsed, fixed with 4% paraformaldehyde, and permeabilized using 0.1% Triton X-100. After washing, cells were blocked for 30 min with 1% BSA in PBS and then were incubated with primary antibodies overnight at 4°C. Then, cells were washed and incubated with fluorescent dye-conjugated secondary antibodies for 1 h at room temperature. The nuclei were stained using DAPI. Fluorescence images were acquired using appropriate optical filters on an AxioImager Z1 ApoTome microscope system (Carl Zeiss, Jena, Germany). Primary antibodies used included anti-CBLL1 (1:100, 21179-1-AP, Proteintech, Wuhan, China), anti-ZC3H13 (1:500, DF4623, Affinity Biosciences, Changzhou, China) and anti-KIF26B (1:1000, 17422-1-AP, Proteintech).

2.4. Cell fractionation and immunoblotting

The cytoplasmic fraction and nuclear fraction of NMFH-1 cells were prepared following the method introduced in one previous study [17]. For western blot analysis, samples were then separated on 10% SDS-PAGE gels, and electrotransferred onto polyvinylidene difluoride (PVDF) membranes (Millipore, Billerica, MA, USA) and subjected to immunoblotting with different antibodies. The blots were then visualized with BeyoECL Star reagent (Beyotime) and an ImageQuant LAS-4000 imaging system (GE Healthcare, Piscataway, NJ, USA). Protein band intensity was quantified using ImageJ software (NIH, USA). Primary antibodies used are provided in Table S2.

2.5. Co-immunoprecipitation (co-IP)

Cells overexpressing KIF26B with N-terminal HA tag (HA-KIF26B) alone or in combination with ZC3H13 with Flag tag (Flag-ZC3H13, full length or truncated ones) or CBLL1 with Flag tag (Flag-CBLL1, full length or truncated ones) were washed once with PBS and lysed in hypotonic buffer and the cytoplasmic fraction was prepared as described above. The cytoplasmic fraction was pre-cleaned by protein A/G PLUS-Agarose (Santa Cruz Biotechnology, Santa Cruz, CA, USA) and the aliquots were immunoprecipitated with a specific antibody against HA tag (ab18181, Abcam), followed by incubation with protein A/G PLUS-Agarose beads for a further 1 h at 4°C. The immunoprecipitated complexes were washed, and the precipitated proteins were then analyzed by western blot analysis (anti-Flag, ab1162, Abcam). Reciprocal IP was performed using the cytoplasmic fraction of untreated cells, with anti-CBLL1 (Cat#A302-969A, Bethyl Laboratories), anti-ZC3H13 (Cat #A300-748A, Bethyl Laboratories) or anti-WTAP (ab195380, Abcam). The input was used as a positive control.

2.6. RNA extraction & qRT-PCR

TRIzol Reagent (Life Technologies, CA, USA) was used to extract total RNA. Then, complementary DNA was reversely transcribed by using the iScript cDNA Synthesis Kit (Bio-Rad, CA, USA). qRT-PCR was performed using an SYBR premix Ex Taq (Takara, Liaoning, China) and ABI 7500 Sequence Detection System (Thermo Fisher Scientific, MA, USA). The primers used were presented in Table S2.

2.7. m6A RNA quantification assay

The m⁶A RNA content in total RNAs was measured with the m⁶A RNA methylation quantification kit (ab185912, Abcam, UK) according to the manufacturer's instructions. Briefly, 200 ng RNAs were coated on the assay wells, followed by adding detection antibody solution and capture antibody solution. Absorbance at 450 nm was recorded to quantify the m⁶A RNA methylation levels. Calculations were conducted based on the standard curve.

2.8. Prediction of KIF26B correlated transcription factors (TFs) and binding of TFs in the KIF26B promoter

The TFs with potential binding to the KIF26B promoter were identified using Cistrome Data Browser (<http://cistrome.org/db/#/>) [18]. Their Pearson's correlation coefficients with KIF26B expression in 60 UPS/MFS and 139 basal-like breast cancer (BLBC) cases in TCGA were calculated. The promoter sequence of *KIF26B* was acquired from the *KIF26B* promoter clone in GeneCopoeia (ID: HPRM49076) (Fig. S3). Then, the promoter sequence was scanned using JASPAR (<http://jaspar.genereg.net/>) to identify the potential binding site (BS) of serum response factor (SRF). The relative profile score threshold was set to 80%.

2.9. Dual-luciferase assay

The full length wild-type (−1223/+193) or mutant *KIF26B* promoter were cloned into pGL3 basic vector (termed as pGL3-KIF26B-promoter-WT and pGL3-KIF26B-promoter-MT). MDA-MB-157 and NMFH-1 cells with or without lentiviral-mediated *SRF* inhibition were seeded in 24-well plates at a density of 2×10^5 cells per well. 24 h later, the cells were transfected with either 1 μg of empty pGL3 basic vector or recombinant constructs using Lipofectamine 2000 (Invitrogen). 0.05 μg of pRL-CMV vector was co-transfected to normalize the transfection efficiency. 48 h later, cells were lysed, and the activities of firefly luciferase and renilla luciferase were quantified using a dual-specific luciferase assay kit according to the manufacturer's instruction (#E1910, Promega).

2.10. Chromatin immunoprecipitation (ChIP)-qPCR

ChIP was conducted using ExactaChIP Chromatin Immunoprecipitation Kits (R&D, Minneapolis, MN, USA), according to the manufacturer's instructions. The lysates were incubated with anti-SRF or IgG. Then, the secondary antibody (goat anti-rabbit IgG-biotin) was added. Immunoprecipitated DNA was collected using magnetic streptavidin beads, purified using a PCR purification kit, and then was used for qRT-PCR. The primers used for ChIP-qPCR were provided in Table S2.

2.11. Gene-specific m6A RIP-qPCR

The Magna methylated RIP (Me-RIP) kit (Millipore, cat. #CR203146) was used to examine m6A modification of *SRF* mRNA according to the manufacturer's instruction and modifications of one previous study [19]. In brief, 100 μg of total RNA sheared to approximately 100 nt in length via metal-ion induced fragmentation and purified. Then, the fragmented RNA was incubated with anti-m6A antibody or mouse IgG (CS200621, Millipore)-conjugated Protein A/G magnetic beads in 500 μl 1x IP buffer supplemented with RNase inhibitors at 4 °C overnight. Methylated RNA was immunoprecipitated with beads, eluted by competition with free m6A, and recovered with RNeasy kit (Qiagen). The RNA enrichment was analyzed by qRT-PCR.

2.12. Cell proliferation and colony formation assay

24 h after lentiviral infection, cells were plated into 96-well culture plates (3000 cells/well) and further cultured for 24, 48, 72, and 96 h. Cell proliferation was measured using Cell Counting Kit-8 (CCK-8, Beyotime, Wuhan, China) according to the manufacturer's protocol. For colony formation assay, cells were seeded into six-well plates (500 cells/well) with three biological repeats for each group. After cultivation for 10 days, cells were fixed with 4% paraformaldehyde, followed by staining with 1% crystal violet for 30 min. Then the colonies were imaged and counted.

2.13. Animal studies

Animal experiments were approved by the Institutional Animal Care and Use Committee of Sichuan Provincial People's Hospital, Chengdu, China. All animal experiments have been conducted following the Institutional Animal Care and Use Committee. BALB/c nude mice (5 weeks old) were purchased from the Beijing HFK Bioscience Co. Ltd. 2×10^6 cells (50 μL) were mixed with 50 μL Matrigel (BD Biosciences, San Jose, CA, USA) were injected subcutaneously in the rear flank fat pad of the nude mice (N = 6, per group). Tumor growth was measured twice weekly using calipers, with the tumor volume (mm³) calculated using the following formula: $V = L (\text{length}) \times W (\text{width})^2/2$.

2.14. Statistical analysis

Data was reported as mean ± SD based on at least three biological replicates. Data integration and statistical analysis were performed using GraphPad Prism 8.1.2 (GraphPad Inc., La Jolla, CA, USA). One-way ANOVA with post hoc Tukey's multiple comparisons test and Welch's unequal variances t-test were conducted. Kaplan-Meier (K-M) curves of RFS/PFS/OS were generated for prognostic comparisons, with log-rank test to detect the difference. $p < 0.05$ was considered statistically significant.

3. Results

3.1. Ginsenoside Rh2 reduces m6A RNA methylation and KIF26B expression in some cancer

Multiple cancer cell lines, including MDA-MB-157, MCF-7 (breast cancer cell lines), KYM1, SK-LMS-1, NMFH-1 (sarcoma cell lines), 8305C, TT (thyroid cancer cell lines), NCIH226, NCIH1299, and NCIH1650 (lung cancer cell lines) were treated with 10 or 20 nM ginsenoside Rh2 for 24 h. m6A RNA methylation in MDA-MB-157, KYM-1, NMFH-1, 8305C, TT and NCIH226 cells was decreased in a ginsenoside Rh2 dose-dependent manner (Fig. 1A). Previous RNA-seq studies in our lab (not shown) identified *KIF26B* is a potential target of ginsenoside Rh2. To validate this finding, the cell lines after treatment in panel A were subjected to qRT-PCR analysis. Ginsenoside Rh2 treatment significantly suppressed the *KIF26B* transcription in multiple cancer cell lines (Fig. 1B).

RNA-seq data from human cancers in TCGA and normal tissues in GTEx showed that *KIF26B* expression varied significantly in different cancers (Fig. S1A). Among the cell lines in panel A, MDA-MB-157, KYM1, NMFH-1, 8305C, TT, and NCIH226 cells had relatively high expression of *KIF26B* protein (Fig. 1C). Ginsenoside Rh2 treatment significant suppressed *KIF26B* protein expression in MDA-MB-157, NMFH-1 and TT cells (Fig. 1D).

Potential proteins that physically interact with *KIF26B* were predicted using GeneMANIA [20] (Fig. S1B). ZC3H13 and CBLL1, two critical proteins involved in m6A RNA methylation [17], triggered our interest. Therefore, we hypothesized that *KIF26B* might also be

a modulator of m6A RNA methylation in cancer. To validate this hypothesis, MDA-MB-157 and NMFH-1 cells were subjected to *KIF26B* inhibition alone or in combination with MT-*KIF26B* (resistant to *KIF26B* shRNA#1 by synonymous mutation) overexpression (Fig. 1E–F). *KIF26B* knockdown reduced m6A RNA methylation in these two cell lines (Fig. 1G–H). Enforced mutant *KIF26B* overexpression significantly restored total m6A RNA methylation level (Fig. 1G–H). Besides, MT-*KIF26B* overexpression also partly reversed ginsenoside Rh2 induced downregulation of m6A RNA levels (Fig. 1I–J).

3.2. *KIF26B* interacts with *ZC3H13* and *CBL1* in the cytoplasmic fraction of cancer cells

IF staining in sarcoma cells in the HPA showed that *KIF26B* mainly locates in the plasma membrane and microtubules (Fig. S1C). In comparison, both *ZC3H13* and *CBL1* distribute in both nuclear and cytoplasm (Fig. S1C). Primary IF staining showed that *KIF26B* was co-localized with *CBL1* and *ZC3H13* in the three cell lines, mainly in the cytoplasm (Fig. 2A). Therefore, Co-IP assay was performed using the cytoplasmic fraction of the three cell lines. Results confirmed the interactions of *KIF26B* with *ZC3H13* and *CBL1* (Fig. 2B, left panel). Negative control panels were provided Fig. S1D–F. In reciprocal IP, *KIF26B* could be pulled down by anti-*CBL1* and anti-*ZC3H13* (Fig. 2B, right panel).

Truncated *ZC3H13* and *CBL1* constructs with an N-terminal Flag-tag were generated (Fig. 2C and D). When the *ZC3H13* constructs were co-expressed with HA-tagged *KIF26B* in NMFH-1 cells, only the constructs containing the central coiled-coil domain (645–789aa), but not other regions, could interact with *KIF26B* (Fig. 2E). When the *CBL1* constructs were co-expressed with HA-tagged *KIF26B*, only the constructs containing the HYB domain (148–206aa), but not other regions, could interact with *KIF26B* (Fig. 2F).

3.3. *KIF26B* enhances nuclear localization of *ZC3H13*/*CBL1*

KIF26B inhibition slightly decreased *ZC3H13* and *CBL1* expression at the mRNA and protein levels (Fig. 3A–D). Interestingly, *KIF26B* inhibition reduced the nuclear fraction of *ZC3H13* and *CBL1*, but increased their cytoplasmic fraction (Fig. 3C–D, Fig. S2A–B). Upon *KIF26B* knockdown, *ZC3H13* and *CBL1* showed a significant decrease in the nuclear part (Fig. 3G). To rule out potential shRNA off-target effects, MT-*KIF26B* (resistant to the shKIF26B#1 sequence) was re-introduced into MDA-MB-157 and NMFH-1 cells with *KIF26B* knockdown. MT-*KIF26B* restored the nuclear distribution of *ZC3H13* and *CBL1* (Fig. 3E–F, Fig. S2C–D), indicating that *KIF26B* indeed modulates the subcellular localization of *ZC3H13* and *CBL1*.

The cytoplasmic localization of *ZC3H13* reduces the nuclear localization of other m6A writer complex components [17]. Since *KIF26B* modulates *ZC3H13* subcellular location, it also might

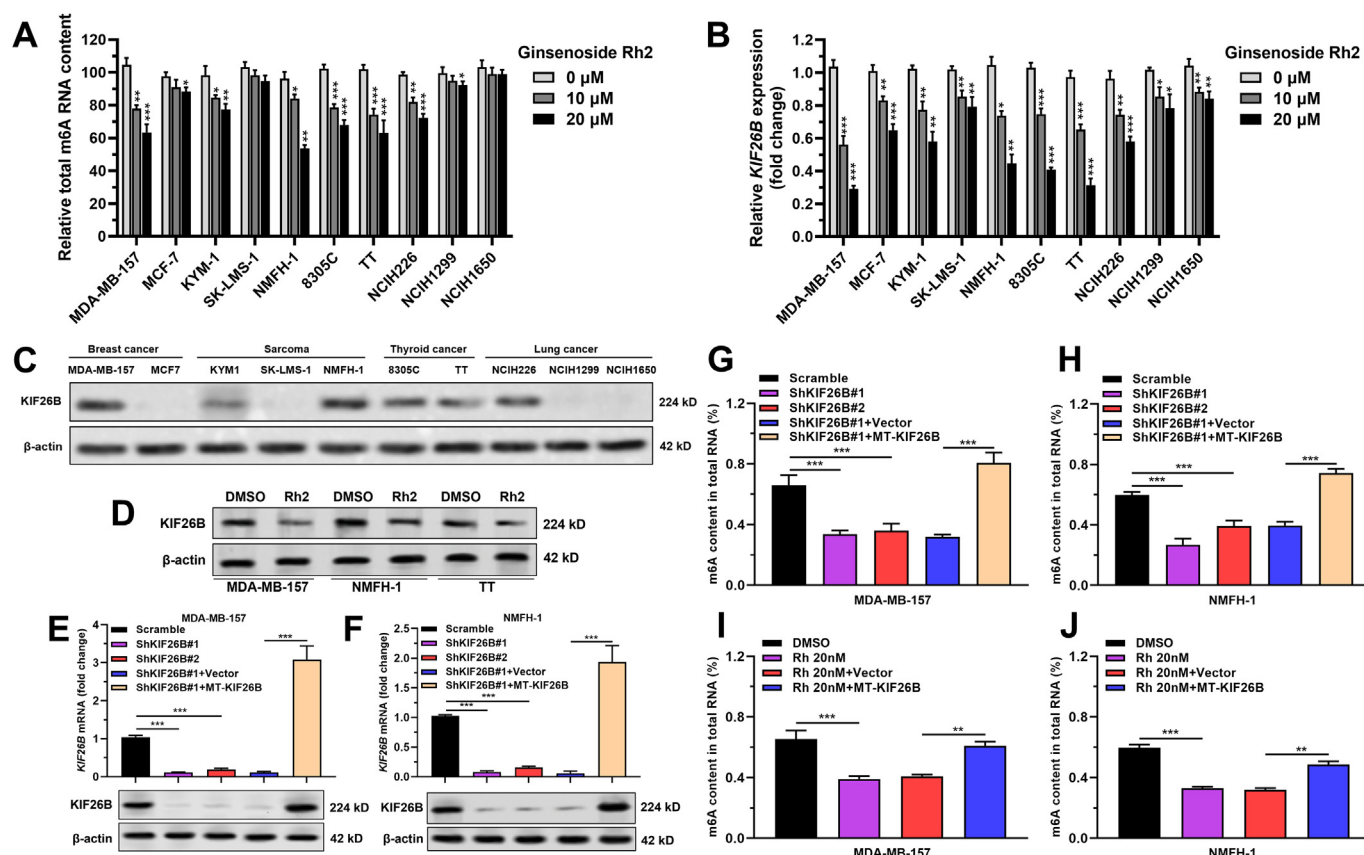


Fig. 1. Ginsenoside Rh2 reduces m6A RNA methylation and *KIF26B* expression in some cancers. **A.** mRNA m6A content in ginsenoside Rh2 treated (10 or 20 nM, 24 h) cancer cell lines. **B.** *KIF26B* mRNA expression in multiple cancer cell lines (the same as in panel A) after treatment with ginsenoside Rh2 (20 nM, 24 h). **C–D.** Basal *KIF26B* protein expression in cancer cell lines as in panel A (C) and in three selected cancer cell lines (MDA-MB-157, NMFH-1, and TT) after treatment with ginsenoside Rh2 (20 nM, 24 h) (D). **E–F.** *KIF26B* mRNA (top panel) and protein (bottom panel) expression in MDA-MB-157 (E) and NMFH-1 (F) cells with lentiviral mediated *KIF26B* knockdown, or in combination with lentiviral *KIF26B* expression vector resistant to shKIF26B#1 (MT-*KIF26B*). **G–J.** mRNA m6A content in *KIF26B* knockdown alone or control MDA-MB-157 (G) and NMFH-1 (H) cells, and in MDA-MB-157 (I) and NMFH-1 (J) cells with ginsenoside Rh2 treatment alone (20 nM, 24 h) or in combination with WT-*KIF26B* overexpression.

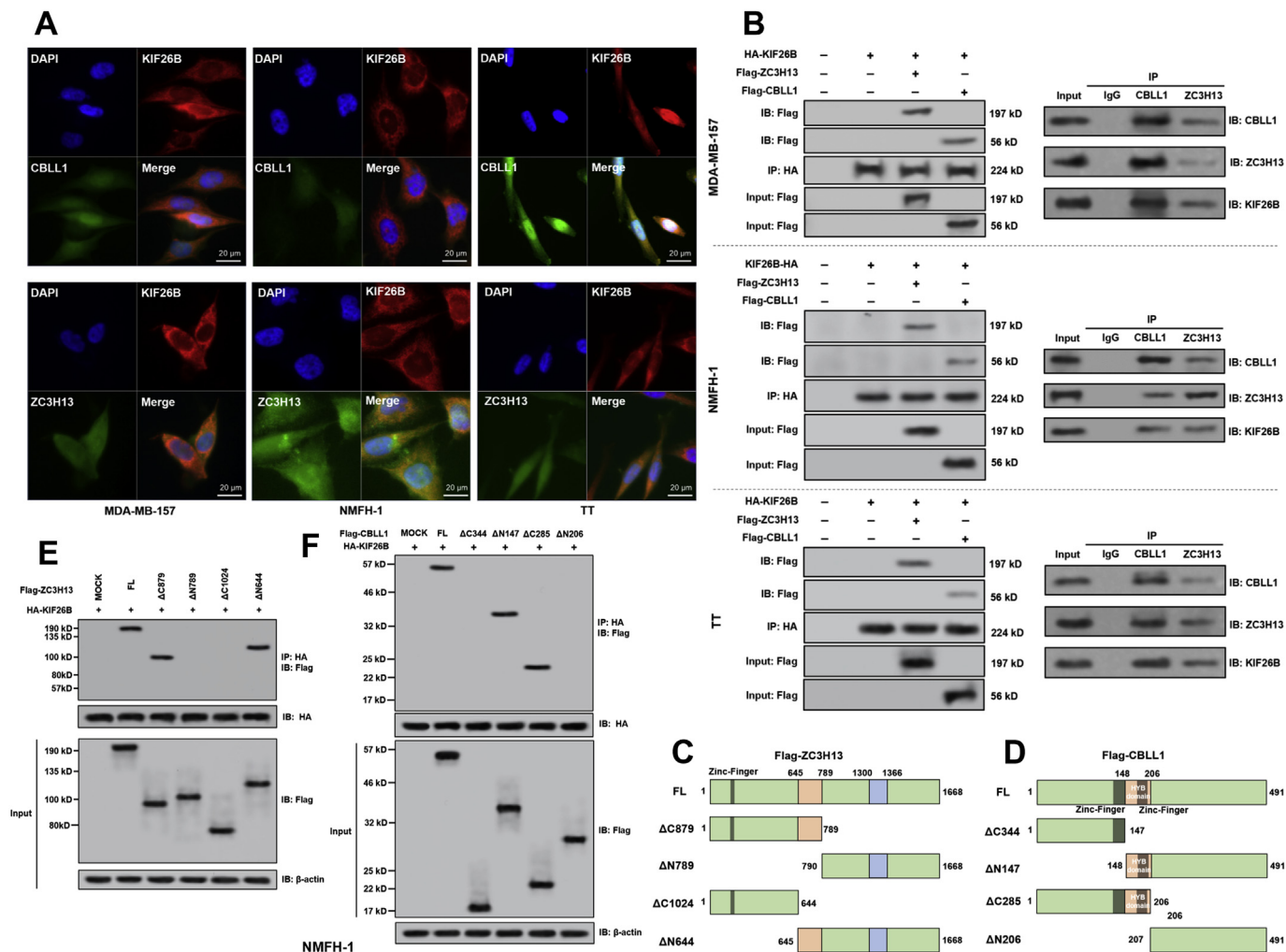


Fig. 2. KIF26B interacts with ZC3H13 and CBLL1 in the cytoplasmic fraction of multiple cancer cell lines. **A.** IF staining of KIF26B (red), CBLL1 (green), and ZC3H13 (green) in MDA-MB-157, NMFH-1 and TT cells. **B.** Left panel, Co-IP was conducted using the cytoplasmic fraction MDA-MB-157 (top), NMFH-1 (middle), and TT (bottom) cells. Right panel, reciprocal IP assay was performed to explore the interaction of ZC3H13 and CBLL1 with KIF26B. KIF26B was immunoprecipitated by anti-CBLL1 and anti-C3H13. **C and D.** The structure of the wild-type full length (FL) and mutation constructs of Flag-tag labeled ZC3H13 (C) and CBLL1 (D). **E and F.** Flag-tagged FL or truncated mutation constructs were co-transfected with HA-KIF26B into NMFH-1 cells. The KIF26B/Flag-tag complexes were immunoprecipitated by anti-HA antibodies. Flag-ZC3H13 (E) and Flag-CBLL1 (F) proteins were detected using anti-Flag antibodies.

modulate the subcellular distribution of other m6A writer complex components. Fractionation assay showed that *KIF26B* knockdown increased the cytoplasmic localization of other m6A writer complex components, including METTL3, METTL14, VIRILIZER, and WTAP (Fig. 3H–I, Fig. S2E–F). Then, co-IP was conducted with anti-WTAP, using the cytoplasmic fraction of NMFH-1 cells with or without *KIF26B* knockdown. Results indicated that the WTAP-METTL3-METTL14 complex and WTAP-CBLL1-VIRILIZER interactions were intact after *KIF26B* knockdown, suggesting that KIF26B only altered their subcellular localization, but not complex formation (Fig. 3J–K).

3.4. SRF activates *KIF26B* expression via binding to its promoter

The transcription factors (TFs) with high-potential binding to the *KIF26B* promoter were identified using ChIP-seq data in Cistrome Data Browser (<http://dbtoolkit.cistrome.org/?specie=hg38&keyword=KIF26B&factor=factor&distance=10k>). 62 potential TFs were identified (Table S1). Since MDA-MB-157 is a triple-negative (TNBC)/basal-B mammary carcinoma cell line and NMFH-1 is a myxofibrosarcoma (MFS) cell line, the correlations

were examined in TCGA-basal-like breast cancer (BLBC) and undifferentiated pleomorphic sarcoma (UPS)/myxofibrosarcoma (MFS) subsets (Fig. 4A). TCGA research indicated that UPS and MFS fall into the same sarcoma subgroup [21]. By setting Pearson's $r \geq 0.3$ as a cutoff value, 15 TFs correlated with *KIF26B* were identified in TCGA-UPS/MFS and 28 TFs correlated with *KIF26B* were identified in TCGA-BLBC (Table S1). There were eight TF genes in the shared subset (Fig. 4A–B). Among them, serum response factor (SRF) has been characterized as a factor contributing to the malignant behaviors of multiple cancers, including breast cancer [22,23] and sarcoma [24]. A high-score potential binding site of SRF was found in the promoter region of *KIF26B* (Fig. S2, Fig. 4C). SRF inhibition (Fig. 4D and F) significantly reduced *KIF26B* expression at both mRNA and protein levels in MDA-MB-157 and NMFH-1 cells (Fig. 4E–F).

Wild-type (WT) and mutant (MT) *KIF26B* promoter sequence (Fig. 4G) were cloned into the pGL3-basic plasmid and transiently transfected into MDA-MB-157 and NMFH-1 cells. Cells transfected with pGL3-KIF26B-promoter-WT had a significantly higher luciferase activity than the cells transfected with pGL3-KIF26B-promoter-MT (Fig. 4H–I). Knockdown of endogenous SRF significantly

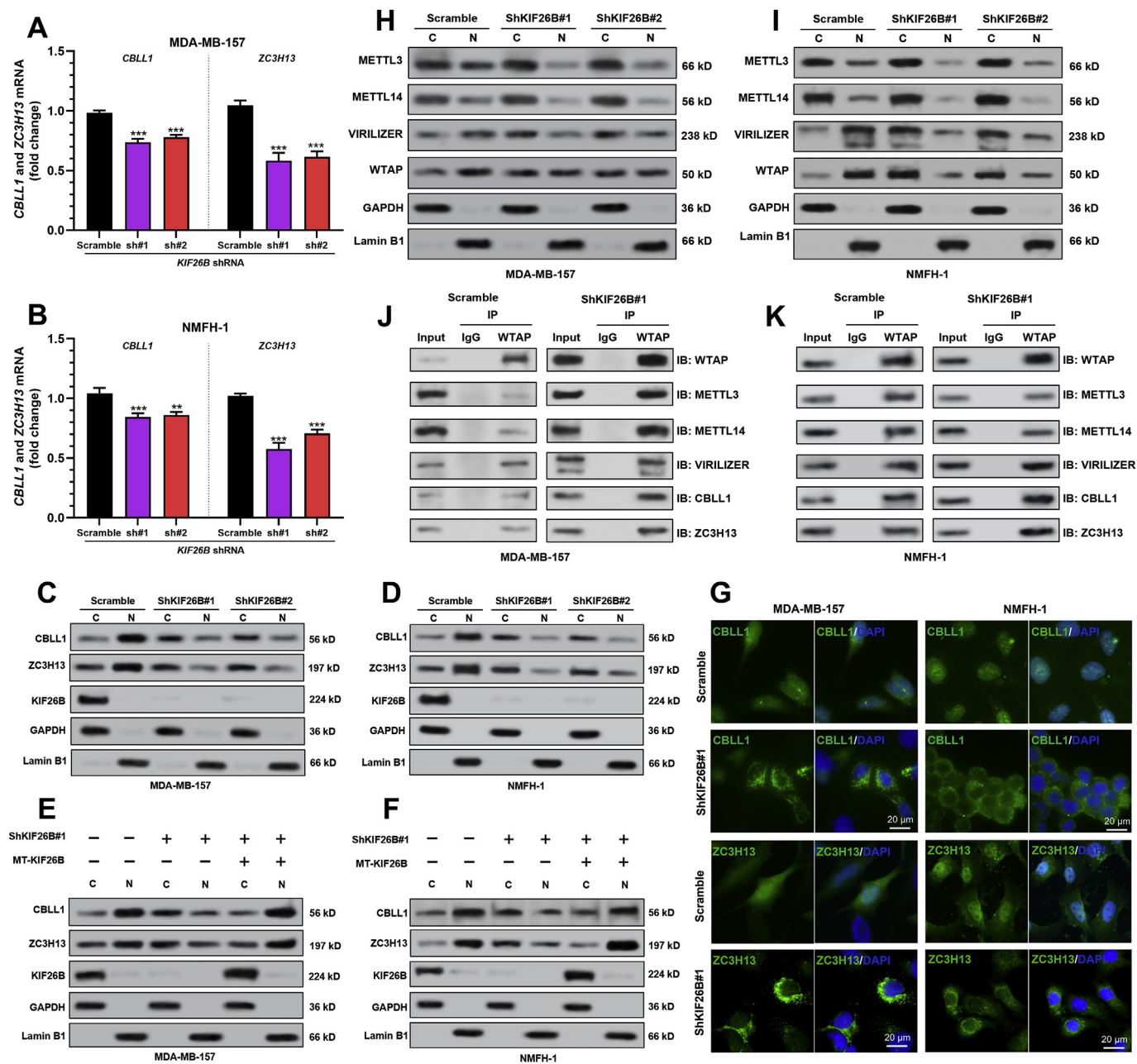


Fig. 3. KIF26B enhances nuclear localization of ZC3H13/CBLL1. **A–B.** *CBLL1* and *ZC3H13* mRNA expression in MDA-MB-157 (A) and NMFH-1 (B) cells with lentiviral mediated *KIF26B* knockdown. **C–F.** *KIF26B*, *ZC3H13*, and *CBLL1* protein expression in the cytoplasmic (C), and nuclear (N) fractions from MDA-MB-157 (panel C and E) and NMFH-1 (panel D and F) cells with *KIF26B* knockdown alone (C–D) or in combination with WT-KIF26B overexpression (E–F). **G.** Immunofluorescence analysis of *CBLL1* (green), *ZC3H13* (green), and DAPI (blue, cell nuclei) in *KIF26B* knockdown and control MDA-MB-157 and NMFH-1 cells. Scale bar, 20 μ m. **H–I.** *METTL3*, *METTL14*, *VIRILIZER*, and *WTAP* protein expression in cytoplasmic (C), and nuclear (N) fractions from MDA-MB-157 (H) and NMFH-1 (I) cells with or without *KIF26B* knockdown. **J–K.** Interactions between *WTAP* and *METTL3*, *METTL14*, *VIRILIZER*, *CBLL1*, and *ZC3H13* were determined by co-IP using cytoplasmic fractions from MDA-MB-157 (J) and NMFH-1 (K) cells with or without *KIF26B* knockdown. n.s., not significant. **, $p < 0.01$; ***, $p < 0.001$.

weakened the luciferase activity of pGL3-KIF26B-promoter-WT, but not pGL3-KIF26B-promoter-MT (Fig. 4H–I). ChIP-qPCR assay data showed that the amplicons covering the SRF binding site, but not the amplicons not covering SRF binding site, were significantly enriched upon anti-SRF immunoprecipitation (Fig. 4J–L).

3.5. SRF mRNA stability was regulated by m6A RNA methylation

The potential m6A modification sites in *SRF* mRNA were checked using SRAMA (<http://www.cuilab.cn/sramp>) [25]. Results identified

four high and very high potential m6A modification sites (Fig. 5A). Gene-specific m6A RIP-qPCR assays showed that m6A abundance in *SRF* mRNA was significantly decreased upon *KIF26B* silencing (Fig. 5B–C). Besides, *KIF26B* knockdown significantly decreased the mRNA and protein levels of *SRF* (Fig. 5D–F), and reduced the stability of *SRF* mRNA in the presence of transcription inhibitor actinomycin D (Fig. 5G–H). These findings revealed a positive feedback regulatory loop between *KIF26B* and *SRF* (Fig. 5I). Since *SRF* itself is an m6A-regulated gene, *KIF26B* might enhance *SRF* expression via regulating *ZC3H13*/*CBLL1* nuclear localization and subsequent m6A

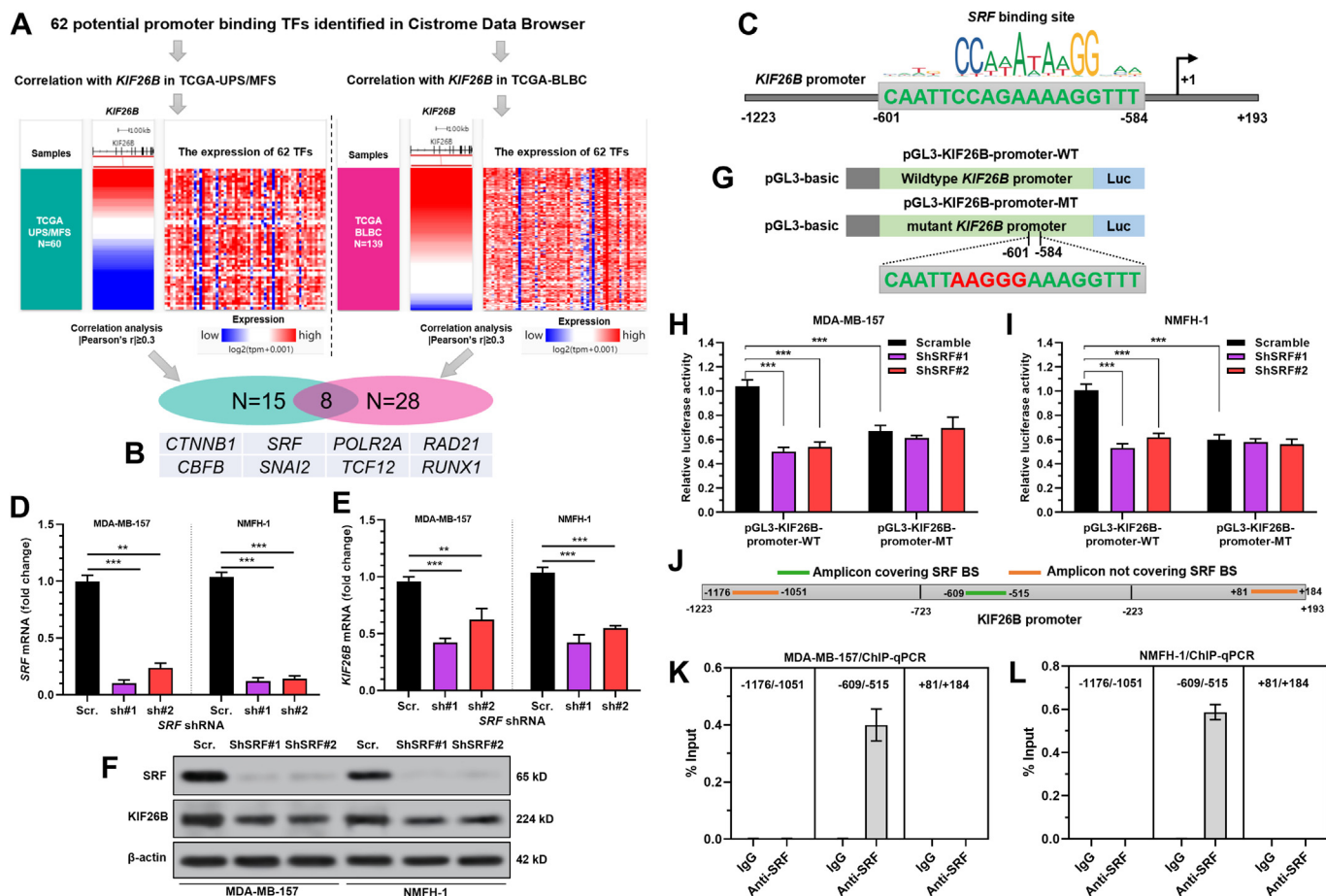


Fig. 4. SRF activates *KIF26B* expression via binding to its promoter. **A–B.** The screening processes and criteria to identify potential TFs ($N = 62$) and their correlation with *KIF26B* expression in 60 UPS/MFS cases and 139 BLBC cases in TCGA. **C.** Predicted binding sites of SRF in the promoter region of *KIF26B*. **D–F.** SRF and *KIF26B* mRNA (D–E) and protein (F) expression in MDA-MB-157 and NMFH-1 cells with lentiviral mediated SRF knockdown. **G.** The structure of pGL3-KIF26B-promoter-WT and pGL3-KIF26B-promoter-MT plasmid for dual-luciferase assay. **H–I.** The promoter activity of the WT and MT *KIF26B* promoter sequence was measured using a dual-luciferase reporter assay. MDA-MB-157 (H) and NMFH-1 (I) cells with or without lentiviral mediated SRF inhibition were co-transfected with pGL3-KIF26B-promoter-WT or pGL3-KIF26B-promoter-MT. **J.** The positions of primers for ChIP-qPCR assay. **K–L.** ChIP-qPCR assays were performed using anti-SRF and control IgG antibodies in MDA-MB-157 (K) and NMFH-1 (L) cells. The relative enrichment was presented as % input. **, $p < 0.01$; ***, $p < 0.001$.

RNA modification. SRF exerts a positive feedback transcriptional activating effect on *KIF26B* expression by promoter binding (Fig. 5I). Ginsenoside Rh2 can decrease m6A RNA level in cancer at least via downregulating *KIF26B* (Fig. 5I).

3.6. SRF-KIF26B axis enhances the growth of cancer cells in vitro and in vivo

SRF or *KIF26B* knockdown significantly suppressed MDA-MB-157 and NMFH-1 cell proliferation and colony formation (Fig. 6A–B, E–H). *KIF26B* overexpression significantly abrogated the suppressive effects of SRF knockdown on cell proliferation and colony formation (Fig. 6C–D, E–H). Animal studies indicated that SRF or *KIF26B* knockdown substantially inhibited MDA-MB-157 and NMFH-1-derived tumor growth *in vivo* and resulted in smaller tumors than the control group (Fig. 6I–L).

Survival data in the Kaplan Meier Plotter (<http://kmplot.com/analysis/>) [26] showed that in TNBC patients, high *KIF26B* expression was associated with significantly shorter recurrence-free survival (RFS) and overall survival (OS) (Fig. 6M–N), while high SRF expression was linked to significantly worse OS, but not RFS (Fig. 6O–P). In patients with UPS/MFS in TCGA, the groups with high *KIF26B* or SRF expression had substantially shorter

progression-free survival (PFS) than the respective low expression groups (Fig. 6Q and S). No difference was observed in OS (Fig. 6R and T).

4. Discussion

The tumor-suppressive effects of ginsenoside Rh2 have been reported in cancers such as breast cancer [5], colon cancer [4], lung cancer [27] and prostate cancer [28]. It induces epigenetic silencing of some tumor-associated genes, such as long non-coding RNA *C3orf67-AS1* [6] and *CASP1*, *INSL5*, and *OR52A1* [5] via promoter hypermethylation. Therefore, the anti-cancer effects of ginsenoside Rh2 might be associated with its epigenetic modulations. The current study showed that ginsenoside Rh2 reduces m6A RNA content in some cancer cells via downregulating *KIF26B* expression. To the best of our knowledge, this is the first study showing the regulatory effect of ginsenoside Rh2 on m6A RNA methylation.

The current study found that *KIF26B* interacted with both ZC3H13 and CBL1 in MDA-MB-157, NMFH-1 and TT cells. ZC3H13 is required for the nuclear localization of WTAP, VIRILIZER, and CBL1, as well as METTL3 and METTL14 [17]. ZC3H13 knockdown remarkably reduces the nuclear speckle localization of these proteins but significantly increased their cytoplasmic localization [17].

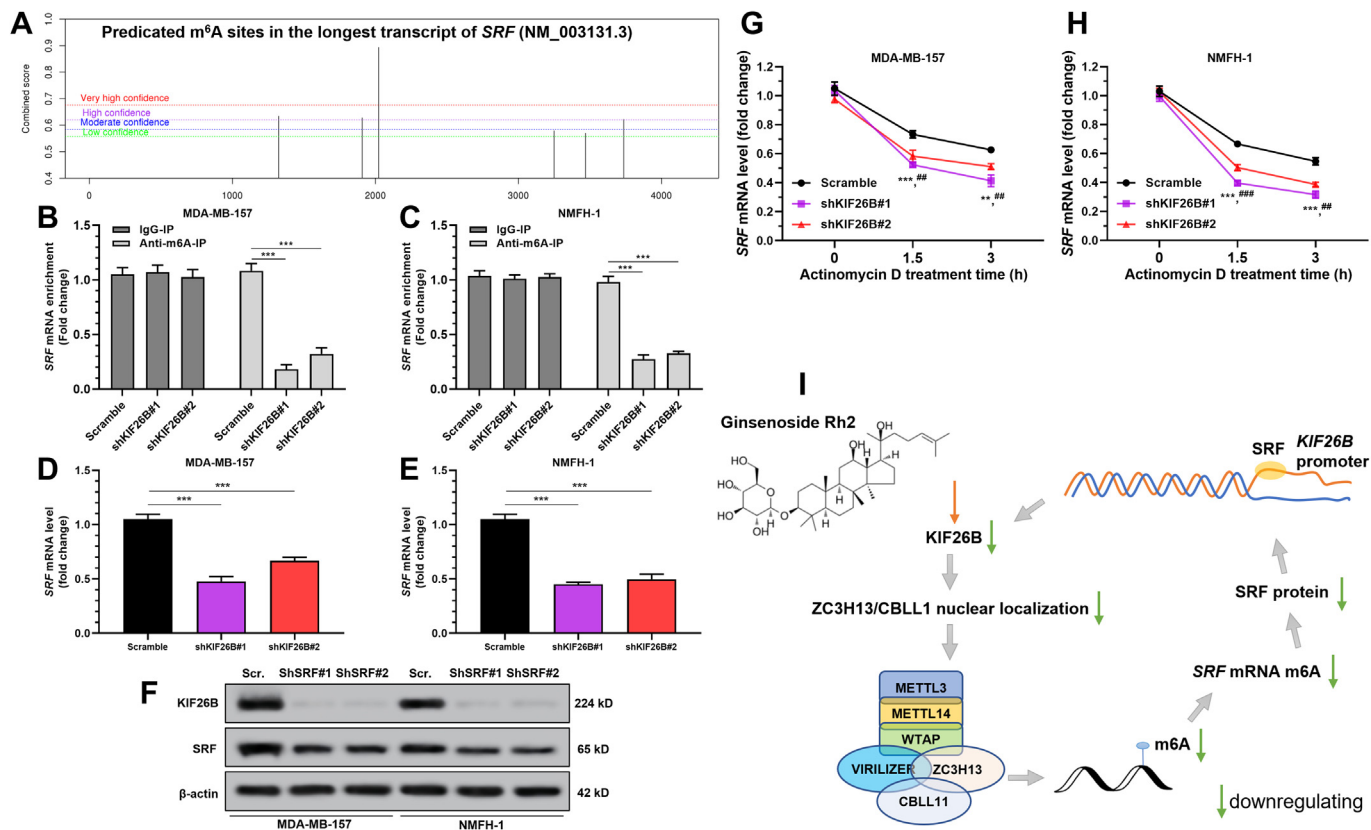


Fig. 5. KIF26B modulates SRF m6A methylation in cancer cells. **A.** Potential m6A modification sites in the sequence of *SRF* mRNA (NM_003131.3). **B–C.** Gene-specific m6A RIP-qPCR assay showing the reduction of m6A modification in specific regions of *SRF* mRNA by shKIF26B in MDA-MB-157 (**B**) and NMFH-1 (**C**) cells. **D–E.** *SRF* mRNA (**D–E**) and protein (**F**) expression in MDA-MB-157 and NMFH-1 cells with lentiviral mediated *KIF26B* knockdown. **G–H.** *SRF* mRNA expression in MDA-MB-157 (**G**) and NMFH-1 (**H**) cells at the indicated time points after actinomycin D treatment. **I.** A potential positive feedback loop between *KIF26B* and *SRF* in cancer cells and the regulatory effect of ginsenoside Rh2 on m6A RNA methylation via *KIF26B*. *, Scramble vs. shKIF26B#1; #, Scramble vs. shKIF26B#2; ## and **, $p < 0.01$; ### and ***, $p < 0.001$.

Knockdown of *KIF26B* also impaired their nuclear localization, as well as the nuclear localization of WTAP, VIRILIZER, METTL3, and METTL14. Since m6A RNA methylation takes place within the nucleus, nuclear entry and speckle localization might be critical for the normal functional role of the m6A writer complex proteins [29]. These findings suggest that *KIF26B* might enhance m6A modification via promoting nuclear localization of ZC3H13 and CBLL1.

M6A modification can destabilize mRNAs via YTHDF2-mediated decay pathway [30]. However, the association between reduced m6A level and decreased RNA stability was also observed [31,32]. One recent study found that IGF2BP1, IGF2BP2, and IGF2BP3 can act as m6A readers, bind to m6A-methylated mRNAs and increase their stability [33]. The current study found that SRF bound to the *KIF26B* promoter and activated its transcription. SRF has been characterized as an oncogenic TF in multiple types of cancers [34–36]. IGFBP1 bindings to m6A modified 3'UTR of *SRF* mRNA and reduces miRNA-mediated decay [37]. Therefore, there might be a reciprocal regulation between *KIF26B* and SRF in cancer. In both MDA-MB-157 and NMFH-1 cells, *KIF26B* knockdown significantly reduced the *SRF* m6A mRNA level and impaired its stability. These findings suggested that *KIF26B* exerts a feedback regulation on *SRF* expression via modulating its m6A modified mRNA level.

Bioinformatic data indicated that five out of the rest seven potential TF genes (*CTNNB1*, *POLR2A*, *RAD21*, *CBFB*, and *TCF12*) in Fig. 4B also have high potential m6A sites (Fig. S4A–G). Therefore, Besides the regulatory effects on *SRF* mRNA stability, *KIF26B* might also regulate the translation or stability of other TF mRNAs.

Knockdown of *SRF* or *KIF26B* significantly impaired the growth of MDA-MB-157 and NMFH-1 cells both *in vitro* and *in vivo*. *KIF26B* overexpression partly rescued the phenotypes impaired by *SRF* knockdown. Therefore, the SRF-KIF26B axis might be an important signaling pathway facilitating tumor growth. This study also has some issues to be solved in the future. Besides regulating the subcellular localization of ZC3H13 and CBLL1, *KIF26B* also positively modulates their expression at both mRNA and protein levels. However, the underlying mechanisms were not investigated in the current study. M6A site prediction showed that both ZC3H13 and CBLL1 mRNAs have multiple very high confident m6A modification sites (Fig. S4H–I). Whether the m6A level influences their stability or translation has not yet been reported.

In conclusion, this study revealed a novel regulatory effect of ginsenoside Rh2 on m6A RNA methylation in cancer via down-regulating *KIF26B* expression. *KIF26B* can enhance ZC3H13/CBLL1 nuclear localization, thereby elevating m6A RNA levels. Besides, the

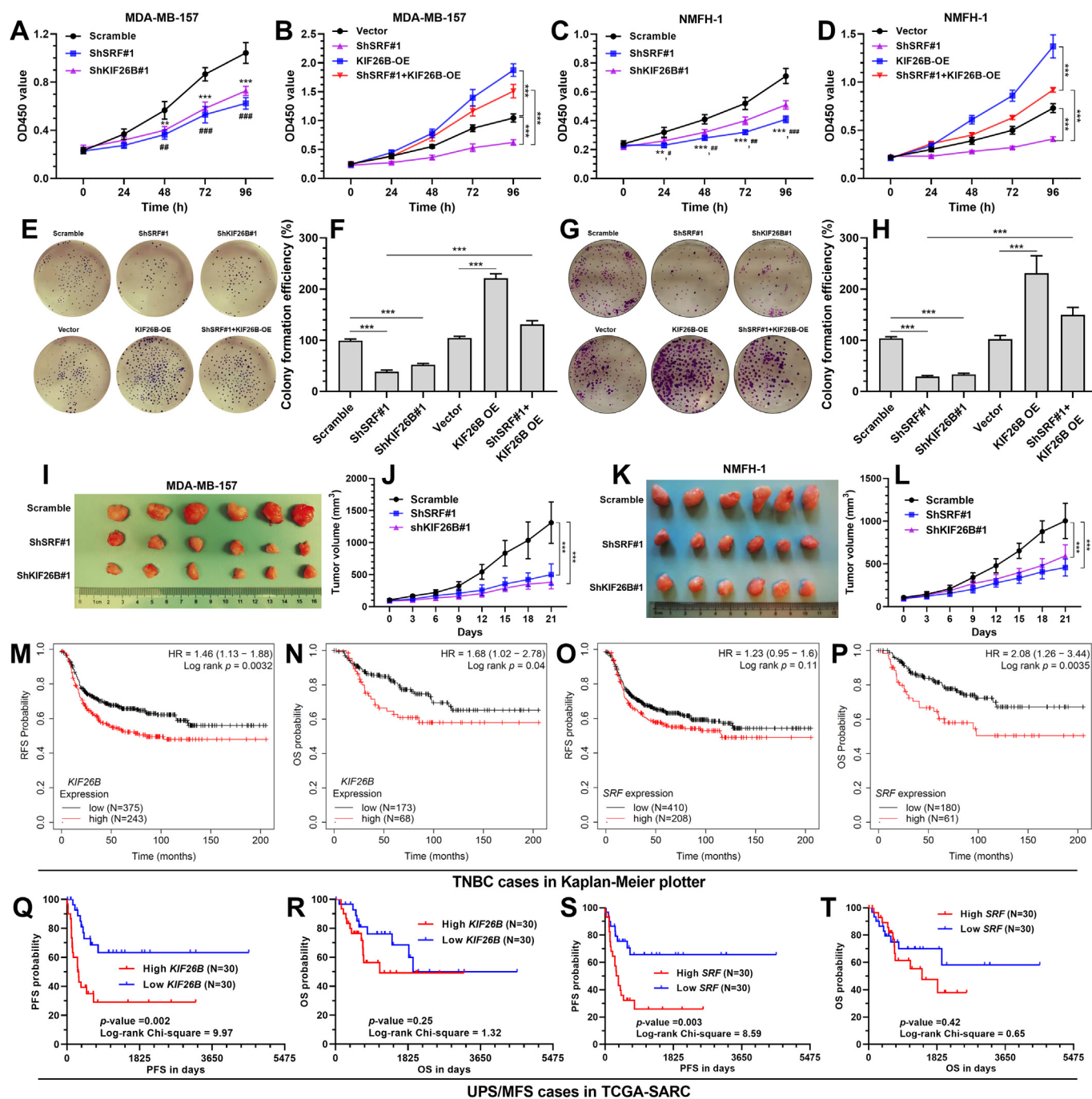


Fig. 6. SRF-KIF26B axis enhances the growth of cancer cells *in vitro* and *in vivo*. **A-D**, Cell proliferation of MDA-MB-157 (A) and NMFH-1 (B) cells with *SRF* or *KIF26B* inhibition alone (A-B) or combined *SRF* inhibition and *KIF26B* overexpression (C-D). **E-H**, Representative images (E and G) and statistical analysis (F and H) of colony formation of MDA-MB-157 (E-F) and NMFH-1 (G-H) cells with *SRF* or *KIF26B* inhibition alone or combined *SRF* inhibition and *KIF26B* overexpression. **I-L**, Representative images of MDA-MB-157 (I-J) and NMFH-1 (K-L) cell (with *SRF* or *KIF26B* inhibition) derived xenograft tumors (I and K) and the growth curves (J and L). **M-T**, Kaplan-Meier survival analysis of RFS and OS in TNBC cases from the Kaplan-Meier plotter (M-P) and PFS and OS in UPS/MFS cases in TCGA-SARC (Q-T). **, $p < 0.01$; ***, $p < 0.001$.

positive feedback regulation between KIF26B and SRF might be an important signaling pathway facilitating tumor growth.

Declaration of competing interest

No potential conflicts of interest are disclosed.

Appendix A. Supplementary data

Supplementary data to this article can be found online at <https://doi.org/10.1016/j.jgr.2021.05.004>.

References

- [1] Mathiyalagan R, Wang C, Kim YJ, Castro-Aceituno V, Ahn S, Subramaniam S, et al. Preparation of polyethylene glycol-ginsenoside Rh1 and Rh2 conjugates and their efficacy against lung cancer and inflammation. *Molecules* 2019;24(23).
- [2] Choi S, Kim TW, Singh SV. Ginsenoside Rh2-mediated G1 phase cell cycle arrest in human breast cancer cells is caused by p15 Ink4B and p27 Kip1-dependent inhibition of cyclin-dependent kinases. *Pharm Res* 2009;26(10):2280–8.
- [3] Li B, Zhao J, Wang CZ, Searle J, He TC, Yuan CS, et al. Ginsenoside Rh2 induces apoptosis and paraptosis-like cell death in colorectal cancer cells through activation of p53. *Cancer Lett* 2011;301(2):185–92.
- [4] Yang J, Yuan D, Xing T, Su H, Zhang S, Wen J, et al. Ginsenoside Rh2 inhibiting HCT116 colon cancer cell proliferation through blocking PDZ-binding kinase/T-LAK cell-originated protein kinase. *J Ginseng Res* 2016;40(4):400–8.
- [5] Lee H, Lee S, Jeong D, Kim SJ. Ginsenoside Rh2 epigenetically regulates cell-mediated immune pathway to inhibit proliferation of MCF-7 breast cancer cells. *J Ginseng Res* 2018;42(4):455–62.
- [6] Jeong D, Ham J, Park S, Kim HW, Kim H, Ji HW, et al. Ginsenoside Rh2 suppresses breast cancer cell proliferation by epigenetically regulating the long noncoding RNA C3orf67-AS1. *Am J Chin Med* 2019;47(7):1643–58.
- [7] Zaccara S, Ries RJ, Jaffrey SR. Reading, writing and erasing mRNA methylation. *Nat Rev Mol Cell Biol* 2019;20(10):608–24.
- [8] Lan Q, Liu PY, Haase J, Bell JL, Huttelmaier S, Liu T. The critical role of RNA m(6)A methylation in cancer. *Cancer Res* 2019;79(7):1285–92.
- [9] Uchiyama Y, Sakaguchi M, Terabayashi T, Inenaga T, Inoue S, Kobayashi C, et al. Kif26b, a kinesin family gene, regulates adhesion of the embryonic kidney mesenchyme. *Proc Natl Acad Sci U S A* 2010;107(20):9240–5.
- [10] Teng Y, Guo B, Mu X, Liu S. KIF26B promotes cell proliferation and migration through the FGF2/ERK signaling pathway in breast cancer. *Biomed Pharmacother* 2018;108:766–73.
- [11] Wang J, Cui F, Wang X, Xue Y, Chen J, Yu Y, et al. Elevated kinesin family member 26B is a prognostic biomarker and a potential therapeutic target for colorectal cancer. *J Exp Clin Cancer Res* 2015;34:13.
- [12] Zhang H, Ma RR, Wang XJ, Su ZX, Chen X, Shi DB, et al. KIF26B, a novel oncogene, promotes proliferation and metastasis by activating the VEGF pathway in gastric cancer. *Oncogene* 2017;36(40):5609–19.
- [13] Dixit D, Prager BC, Gimple RC, Poh HX, Wang Y, Wu Q, et al. The RNA m6A reader YTHDF2 maintains oncogene expression and is a targetable dependency in glioblastoma stem cells. *Cancer Discov* 2020.
- [14] Vu LP, Pickering BF, Cheng Y, Zaccara S, Nguyen D, Minuesa G, et al. The N(6)-methyladenosine (m(6)A)-forming enzyme METTL3 controls myeloid differentiation of normal hematopoietic and leukemia cells. *Nat Med* 2017;23(11):1369–76.
- [15] Tang Z, Kang B, Li C, Chen T, Zhang Z. GEPIA2: an enhanced web server for large-scale expression profiling and interactive analysis. *Nucleic Acids Res* 2019.
- [16] Goldman MJ, Craft B, Hastie M, Repecka K, McDade F, Kamath A, et al. Visualizing and interpreting cancer genomics data via the Xena platform. *Nat Biotechnol* 2020;38(6):675–8.
- [17] Wen J, Lv R, Ma H, Shen H, He C, Wang J, et al. Zc3h13 regulates nuclear RNA m(6)A methylation and mouse embryonic stem cell self-renewal. *Mol Cell* 2018;69(6):1028–10238 e6.
- [18] Zheng R, Wan C, Mei S, Qin Q, Wu Q, Sun H, et al. Cistrome Data Browser: expanded datasets and new tools for gene regulatory analysis. *Nucleic Acids Res* 2019;47(D1):D729–35.
- [19] Weng H, Huang H, Wu H, Qin X, Zhao BS, Dong L, et al. METTL14 inhibits hematopoietic stem/progenitor differentiation and promotes leukemogenesis via mRNA m(6)A modification. *Cell Stem Cell* 2018;22(2):191–205 e9.
- [20] Montojo J, Zuberi K, Rodriguez H, Bader GD, Morris Q. GeneMANIA: fast gene network construction and function prediction for Cytoscape 2014;3:153.F1000Res.
- [21] Cancer Genome Atlas Research Network. Electronic address edsc, cancer Genome Atlas research N. Comprehensive and integrated genomic characterization of adult soft tissue sarcomas. *Cell* 2017;171(4):950–965 e28.
- [22] Kim T, Lim DS. The SRF-YAP-IL6 axis promotes breast cancer stemness. *Cell Cycle* 2016;15(10):1311–2.
- [23] Kim T, Yang SJ, Hwang D, Song J, Kim M, Kyum Kim S, et al. A basal-like breast cancer-specific role for SRF-IL6 in YAP-induced cancer stemness. *Nat Commun* 2015;6:10186.
- [24] Villalca RA, Silveira SM, Barros-Filho MC, Marchi FA, Domingues MA, Scapulatempo-Neto C, et al. Gene expression profiling in leiomyosarcomas and undifferentiated pleomorphic sarcomas: SRC as a new diagnostic marker. *PLoS One* 2014;9(7):e102281.
- [25] Zhou Y, Zeng P, Li YH, Zhang Z, Cui Q. SRAMP: prediction of mammalian N6-methyladenosine (m6A) sites based on sequence-derived features. *Nucleic Acids Res* 2016;44(10):e91.
- [26] Gyorffy B, Lanczky A, Eklund AC, Denkert C, Budczies J, Li Q, et al. An online survival analysis tool to rapidly assess the effect of 22,277 genes on breast cancer prognosis using microarray data of 1,809 patients. *Breast Cancer Res Treat* 2010;123(3):725–31.
- [27] Jin X, Yang Q, Cai N, Zhang Z. A cocktail of betulinic acid, parthenolide, honokiol and ginsenoside Rh2 in liposome systems for lung cancer treatment. *Nanomedicine (Lond)* 2020;15(1):41–54.
- [28] Wang J, Bian S, Wang S, Yang S, Zhang W, Zhao D, et al. Ginsenoside Rh2 represses autophagy to promote cervical cancer cell apoptosis during starvation. *Chin Med* 2020;15(1):118.
- [29] Ping XL, Sun BF, Wang L, Xiao W, Yang X, Wang WJ, et al. Mammalian WTAP is a regulatory subunit of the RNA N6-methyladenosine methyltransferase. *Cell Res* 2014;24(2):177–89.
- [30] Wang X, Lu Z, Gomez A, Hon GC, Yue Y, Han D, et al. N6-methyladenosine-dependent regulation of messenger RNA stability. *Nature* 2014;505(7481):117–20.
- [31] Li Z, Weng H, Su R, Weng X, Zuo Z, Li C, et al. FTO plays an oncogenic role in acute myeloid leukemia as a N(6)-methyladenosine RNA demethylase. *Cancer Cell* 2017;31(1):127–41.
- [32] Yan G, Yuan Y, He M, Gong R, Lei H, Zhou H, et al. m(6)A methylation of precursor-miR-320/RUNX2 controls osteogenic potential of bone marrow-derived mesenchymal stem cells. *Mol Ther Nucleic Acids* 2020;19:421–36.
- [33] Huang H, Weng H, Sun W, Qin X, Shi H, Wu H, et al. Recognition of RNA N(6)-methyladenosine by IGF2BP proteins enhances mRNA stability and translation. *Nat Cell Biol* 2018;20(3):285–95.
- [34] Zhao X, He L, Li T, Lu Y, Miao Y, Liang S, et al. SRF expedites metastasis and modulates the epithelial to mesenchymal transition by regulating miR-199a-5p expression in human gastric cancer. *Cell Death Differ* 2014;21(12):1900–13.
- [35] Liu CY, Chan SW, Guo F, Toloczko A, Cui L, Hong W. MRTF/SRF dependent transcriptional regulation of TAZ in breast cancer cells. *Oncotarget* 2016;7(12):13706–16.
- [36] Wang HY, Zhang B, Zhou JN, Wang DX, Xu YC, Zeng Q, et al. Arsenic trioxide inhibits liver cancer stem cells and metastasis by targeting SRF/MCM7 complex. *Cell Death Dis* 2019;10(6):453.
- [37] Muller S, Glass M, Singh AK, Haase J, Bley N, Fuchs T, et al. IGF2BP1 promotes SRF-dependent transcription in cancer in a m6A- and miRNA-dependent manner. *Nucleic Acids Res* 2019;47(1):375–90.